iScience

CellPress
OPEN ACCESS

Article

Etomoxir repurposed as a promiscuous fatty acid mimetic chemoproteomic probe

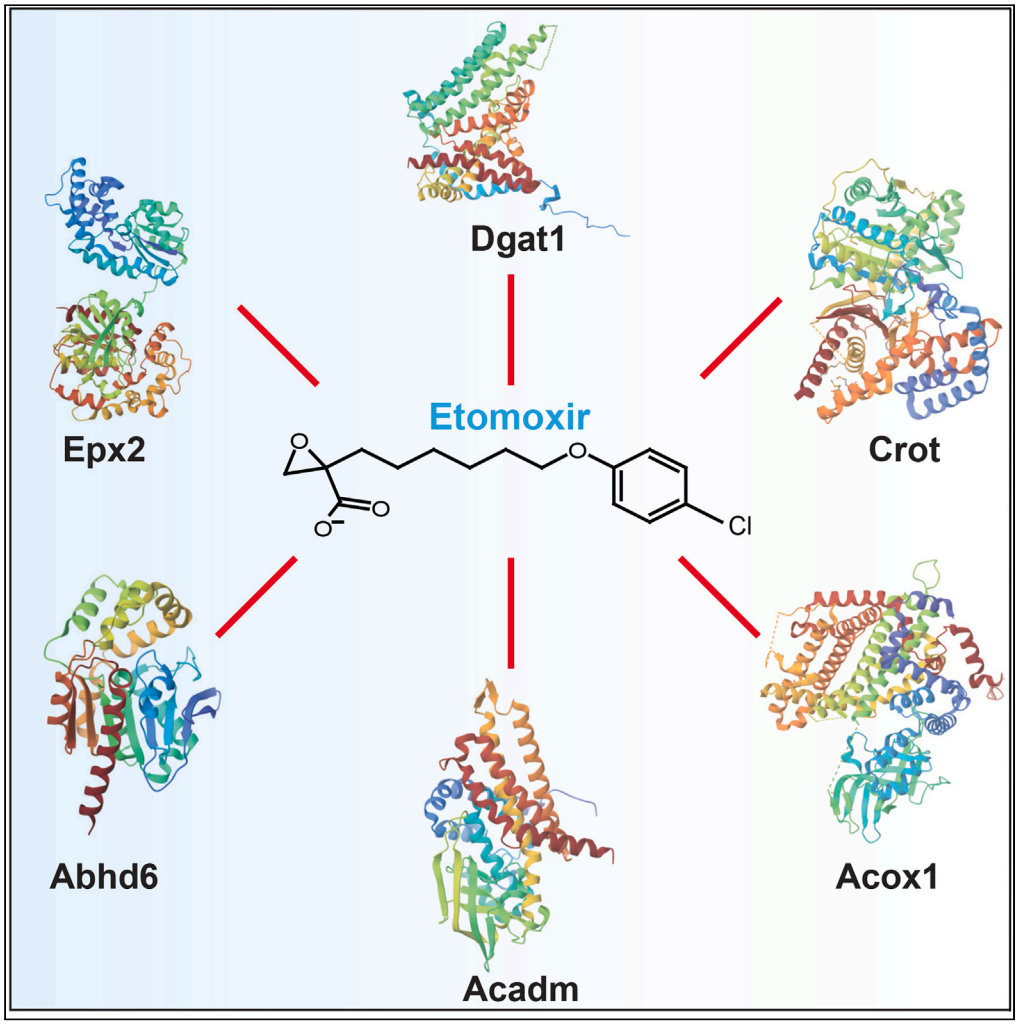

Joseph Choi, Danielle M. Smith, Ye Jin Lee, ..., Susanna Scafidi, Ryan C. Riddle, Michael J. Wolfgang

mwolfga1@jhmi.edu

Highlights

Etomoxir affects lipid metabolism beyond inhibition of fatty acid oxidation

Etomoxir binds a large and diverse array of proteins throughout the cell

Etomoxir concentrates in peroxisomes rather than mitochondria

Etomoxir identifies proteins in an activity-dependent manner

Choi et al., iScience 27, 110642
September 20, 2024
https://doi.org/10.1016/j.isci.2024.110642

iScience

CellPress
OPEN ACCESS

Article

Etomoxir repurposed as a promiscuous fatty acid mimetic chemoproteomic probe

Joseph Choi,[1,2] Danielle M. Smith,[1,2] Ye Jin Lee,[6] Danfeng Cai,[6] Mohammad J. Hossain,[2] Tamara J. O'Connor,[2] Pragney Deme,[4] Norman J. Haughey,[4] Susanna Scafidi,[5] Ryan C. Riddle,[7,8] and Michael J. Wolfgang[1,2,3,9,*]

SUMMARY

Etomoxir has been used for decades as a popular small molecule inhibitor of carnitine palmitoyltransferase I, Cpt1, to block mitochondrial fatty acid β-oxidation. To test the specificity of etomoxir, we generated click chemistry–enabled reagents to label etomoxir binding proteins *in situ*. Etomoxir bound to Cpt1, but also bound to a large array of diverse proteins that metabolize and transport fatty acids in the cytoplasm, peroxisome, and mitochondria. Many of the most abundant proteins identified in primary hepatocytes were peroxisomal proteins. The loss of Pex5, required for the import of peroxisomal matrix proteins, eliminated many of these etomoxir-labeled proteins. By utilizing the promiscuous, covalent, and fatty acid mimetic properties of etomoxir, etomoxir targets of fatty acid ω-oxidation were revealed following the loss of Pex5. These data demonstrate that etomoxir is not specific for Cpt1 and is not appropriate as a tool to distinguish the biological effects of fatty acid oxidation.

INTRODUCTION

Mitochondrial long chain fatty acid β-oxidation is an important central carbon pathway that is critical for many diverse cell types to properly energize cellular function. This is made evident by inborn errors in fatty acid oxidation that result in serious disease.[1] Metabolic crisis becomes apparent following times of food withdrawal when fatty acids, stored as energetically dense triglyceride, supplant other major macronutrients and become the dominant fuel. Beyond simply supplying substrates for ATP generation, fatty acid oxidation has been implicated in processes such as cellular signaling, epigenetic regulation, and posttranslational regulation. These functions have led to suggestions that fatty acid oxidation can affect diverse physiology such as aging, immunity, and cancer progression.[2–4]

The biochemistry of mitochondrial long chain fatty acid β-oxidation has been elucidated in great depth. Exogenous or *de novo* synthesized fatty acids must first be activated by CoA esterification to trap fatty acids, allow aqueous miscibility, and enable acyltransferase reactions via their thioester linkage. Subsequent fatty acid oxidation is regulated by access to enzymes in the peroxisomal or mitochondrial matrix. Mitochondrial transport of long chain acyl-CoAs is regulated by the sequential reactions of the cytoplasmic facing carnitine palmitoyltransferase 1 (Cpt1) and the matrix facing carnitine palmitoyltransferase 2 (Cpt2). Cpt1, the rate limiting step, exchanges CoA for the amino acid carnitine. The resultant acylcarnitine can then traverse the mitochondrial inner membrane via the carnitine/acylcarnitine translocase. Cpt2 then exchanges carnitine for CoA so that the reformed acyl-CoA is available to the β-oxidation machinery. Cpt1 is encoded by two genes, Cpt1a and Cpt1b, that demonstrate tissue selectivity while Cpt2 is encoded by a single gene that is expressed ubiquitously.

Research into fatty acid oxidation has been dominated for >40 years by the small molecule inhibitor etomoxir.[5] Etomoxir is often described as a specific inhibitor of Cpt1 and is used to demonstrate and isolate the biological effects of mitochondrial fatty acid β-oxidation to this single step. Intuitively, the structure of etomoxir does not suggest specificity. It is an epoxide containing medium chain fatty acid that is itself CoA esterified by cellular Acyl-CoA Synthetases. Recently, several long held dogmas of fatty acid oxidation have been called into question as the genetic loss of fatty acid oxidation does not phenocopy etomoxir treatment and etomoxir retains its biological activity even when its putative targets are absent.[6–11] This suggests that this ubiquitous and heavily utilized small molecule inhibitor has other significant unknown cellular targets.

In order to understand the full biological impact of etomoxir, we generated Click ready etomoxir probes. Click-etomoxir retains its inhibitory effect on fatty acid oxidation, but abundantly labels numerous proteins in cells *in vitro* and *in vivo*. In fact, etomoxir's on-target Cpt1a is

[1]Department of Physiology, The Johns Hopkins University School of Medicine, Baltimore, MD, USA
[2]Department of Biological Chemistry, The Johns Hopkins University School of Medicine, Baltimore, MD, USA
[3]Department of Pharmacology and Molecular Sciences, The Johns Hopkins University School of Medicine, Baltimore, MD, USA
[4]Department of Neurology, The Johns Hopkins University School of Medicine, Baltimore, MD, USA
[5]Department of Anesthesiology and Critical Care Medicine, The Johns Hopkins University School of Medicine, Baltimore, MD, USA
[6]Department of Biochemistry and Molecular Biology, Johns Hopkins Bloomberg School of Public Health, Baltimore, MD, USA
[7]Department of Orthopaedics, University of Maryland School of Medicine, Baltimore, MD, USA
[8]Research and Development Service, Baltimore VA Medical Center, Baltimore, MD, USA
[9]Lead contact
*Correspondence: mwolfga1@jhmi.edu
https://doi.org/10.1016/j.isci.2024.110642

completely obscured by other proteins in the liver and primary hepatocytes. Proteomics in primary hepatocytes demonstrates Cpt1a binding but also promiscuous binding to proteins known to metabolize and transport fatty acids throughout the cell. Unexpectedly, etomoxir binds to a large number of peroxisomal proteins and localizes to peroxisomes *in situ*. The loss of the peroxisomal matrix import protein, Pex5, in primary hepatocytes eliminates etomoxir binding to many of these proteins and reveals unique targets. These data show the highly promiscuous nature of this often-described specific inhibitor, but also demonstrates the utility of etomoxir as a fatty acid mimetic that can be used to discover unique fatty acid biochemistry.

RESULTS

While etomoxir has often been described as a specific inhibitor of Cpt1, its structure and highly reactive epoxide moiety suggests a more promiscuous set of targets. We and others have shown that several hitherto important biological activities of etomoxir cannot be explained solely by the inhibition of Cpt1 or fatty acid oxidation, as the biological effects are retained in Cpt1/Cpt2 knockout tissues and cells.[6–11] In order to define etomoxir binding proteins in cells, we generated unique etomoxir analogues that have replaced the terminal chloride with an alkyne or azido group that reacts with azide and alkyne Click reagents respectively (Figure 1A). The addition of the azide or alkyne would not be expected to impact the Cpt1 inhibitor activity of etomoxir based on previous medicinal chemistry.[5] To test this, we stably expressed a Trimethoprim (TMP) inducible Cpt1a in HEK293T cells. While TMP induced the cells' ability to oxidize fatty acids, etomoxir and both etomoxir Click reagents blocked the cells' ability to fully oxidize radiolabeled oleic acid (Figure 1B). These data show that the Click-etomoxir analogues retain their ability to inhibit fatty acid oxidation.

In order to examine etomoxir and Click-etomoxir in a cell that exhibits robust fatty acid oxidation in a more physiological context, we isolated primary mouse hepatocytes and incubated them for 14 h with 60μM palmitate and 120μM oleate conjugated to fatty acid free BSA in the presence of vehicle, 100μM etomoxir, or etomoxir-alkyne. Consistent with the inhibition of radiolabeled fatty acid oxidation, etomoxir and etomoxir-alkyne inhibited the generation of long chain acylcarnitines and increased their nonesterified free fatty acid analogues (Figure 1C; Table S1). Given that etomoxir inhibits Cpt1 and Cpt1a is the dominant isoenzyme in hepatocytes, we also isolated primary hepatocytes from Cpt1a liver specific KO mice. Etomoxir and etomoxir-alkyne had an even greater effect on long chain acylcarnitines and free fatty acids than in wild-type hepatocytes suggesting additional etomoxir targets of fatty acid metabolism than Cpt1a alone. To gain a broader understanding of the role of etomoxir in fatty acid biochemistry, we performed lipidomics on these samples (Figure 1D; Table S1). These data show that etomoxir and etomoxir-alkyne exhibit similar metabolic effects. Notably, lipidomics in Cpt1a deficient hepatocytes pointed to additional roles of etomoxir in lipid metabolism beyond inhibition of Cpt1 alone.

In order to examine the additional effects of etomoxir, we labeled primary mouse hepatocytes for 24hrs with both etomoxir analogues at 100μM, a common concentration used throughout the literature, and visualized etomoxir binding proteins by SDS-PAGE. Incredibly, a large number of proteins were labeled in primary hepatocytes by both Click analogues (Figure 1E). It has recently been suggested that simply lowering the concentration of etomoxir improves its specificity.[8] Therefore, we lowered the concentration in a dose-dependent manner but we did not observe any improvement in binding specificity (Figure 1F). Next, we demonstrated Click-etomoxir binding could be competed for binding with commercially available etomoxir, demonstrating, along with the metabolic characterization, that Click-etomoxir is binding to *bona fide* etomoxir targets (Figure 1G). Finally, we localized Click-etomoxir *in situ* in primary hepatocytes which demonstrated robust punctate localization (Figure 1H). These results show that rather than a specific inhibitor, etomoxir promiscuously binds to a diverse set of proteins.

Fatty acid oxidation plays numerous important roles in mammalian physiology. To determine if Click-etomoxir could be used to label tissues/proteins *in vivo*, we injected Click-etomoxir into C57BL/6J mice. Tissues were then collected and proteins were separated and visualized by SDS-PAGE. The liver and kidney showed the highest proportion of proteins bound to Click-etomoxir (Figure S1). Intriguingly, heart and skeletal muscle demonstrated a band that overlapped with the molecular weight of Cpt1b (Figure 2A). To test if Click-etomoxir was identifying Cpt1b, we injected mice with a skeletal muscle specific KO of Cpt1b ($Cpt1b^{SKM-/-}$) with Click-etomoxir. Indeed, the band corresponding to Cpt1b bound to Click-etomoxir disappeared in $Cpt1b^{SKM-/-}$ compared to their littermate controls (Figure 2B). While Click-etomoxir binding to Cpt1b can be observed in muscle, it is nonetheless still not specific as many etomoxir binding proteins remain. To determine if one of the many etomoxir binding proteins in the liver corresponds to Cpt1a, we injected mice with a liver specific KO of Cpt1a with Click-etomoxir. Here, we could not identify a loss of Cpt1a in the liver when compared to their littermate controls (Figure 2C). Etomoxir bound too many proteins in the liver, obscuring the loss of Cpt1a. Finally, localizing Click-etomoxir in liver sections of wild-type mice demonstrated robust punctate localization (Figure 2D) similar to primary hepatocytes (Figure 1H). These data show that Click-etomoxir can be used *in vivo* but does not support the specificity of etomoxir.

Etomoxir bound so many proteins in the liver, the genetic loss of Cpt1a could not be observed. Therefore, none of the top etomoxir binding proteins in the liver are Cpt1. In order to identify the proteins in hepatocytes labeled by Click-etomoxir, we replaced the TAMRA probes with biotin. We then isolated proteins bound specifically to Click-etomoxir on streptavidin beads and sequenced trypsin digested proteins by LC-MS/MS. We identified proteins with high confidence, including the on-target Cpt1a, that bound covalently to Click-etomoxir (Figure 3A; Tables S2 and S3). The identity of etomoxir binding proteins was overwhelmingly related to fatty acid metabolism in the peroxisome, mitochondria and cytoplasm. We validated a subset of these proteins by targeted immunoprecipitation (IP) and western blot analysis for the mitochondrial proteins Cpt1a, Hadha and Acadm (Figure 3B) and peroxisomal proteins Acox1 and Crot (Figure 3C). Collectively, these data clearly indicate the spectrum of etomoxir binding proteins, including their subcellular localization is broad.

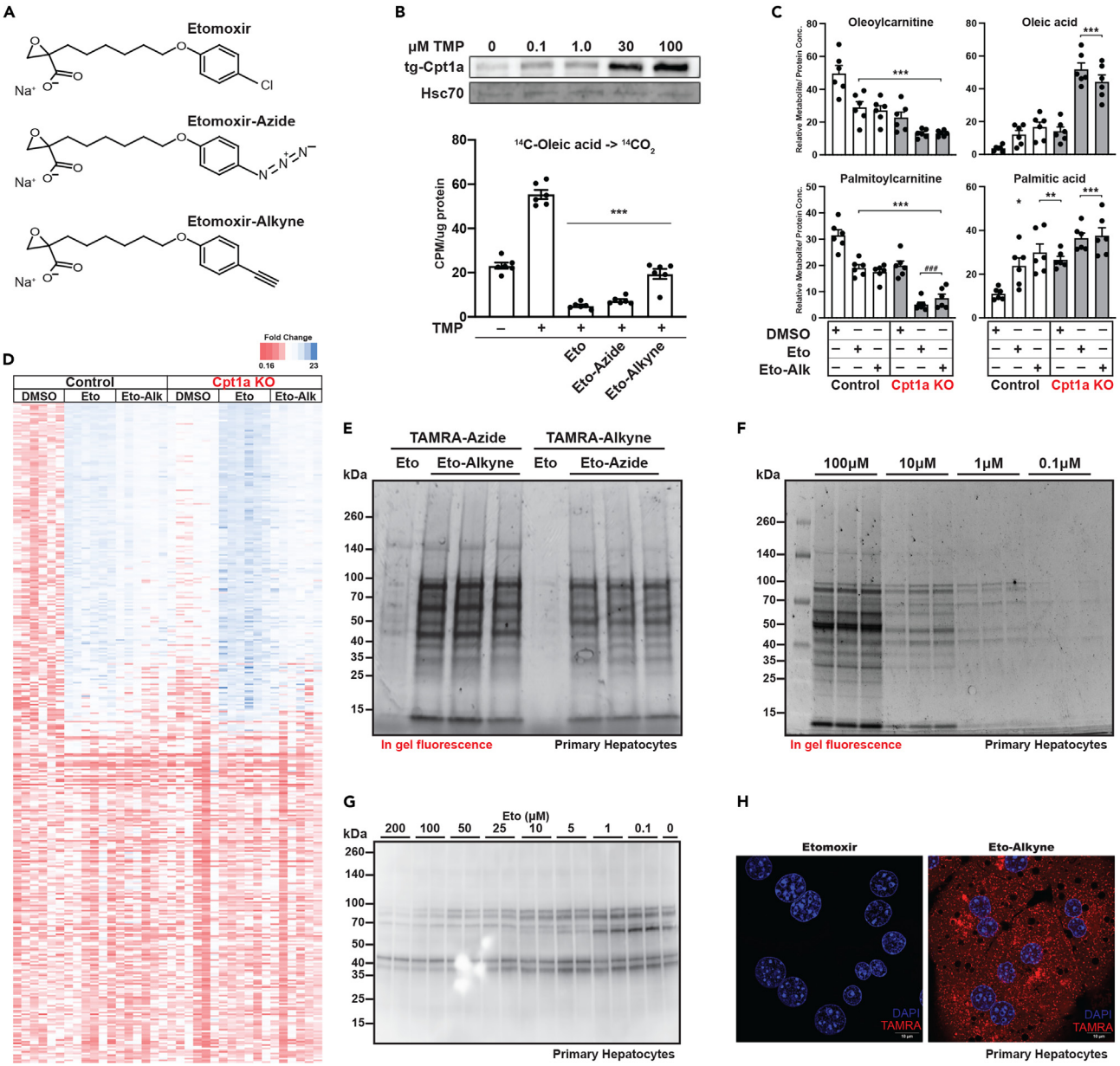

Figure 1. Click-enabled etomoxir inhibits fatty acid oxidation but promiscuously binds an array of proteins

(A) Structures of etomoxir, etomoxir-azide, and etomoxir-alkyne.

(B) Etomoxir (Eto) and Click etomoxir inhibit fatty acid oxidation in HEK293T cells stably expressing TMP-dependent Cpt1a.

(C and D) Acylcarnitine and fatty acid analysis or D. Untargeted lipidomic analysis of primary hepatocytes from wild-type or Cpt1a liver-specific KO mice treated with vehicle, 100μM etomoxir or etomoxir-alkyne in the presence of 60μM palmitate and 120μM oleate.

(E) In gel fluorescence of primary mouse hepatocytes labeled with 100μM Click etomoxir for 24hrs.

(F) Western analysis of dose-dependent labeling in primary mouse hepatocytes treated with 100μM etomoxir-alkyne for 24hrs and labeled with TAMRA-azide and probed for TAMRA.

(G) Etomoxir competes for binding of Etomoxir-alkyne targets. Western blot for TAMRA in primary hepatocytes prelabeled with Etomoxir from 200 to 0 μM competes for binding of Etomoxir-alkyne 0.1μM for 2 h.

(H) Primary hepatocytes showing the localization of Click-etomoxir *in situ*. Scale bar: 10μm. Data are expressed as mean ± SEM. *$p < 0.05$; **$p < 0.01$; ***$p < 0.001$. WT DMSO vs. treatments; ###$p < 0.001$. Cpt1aKO DMSO vs. Etomoxir.

We were surprised by the number and intensity of peroxisomal proteins that were binding to Click-etomoxir. To verify the proteins identified by SDS-PAGE analysis were indeed peroxisomal, we labeled control and Pex5 KO RAW 264.7 cells with Click-etomoxir. Pex5 is required for peroxisomal protein import and its loss disrupts peroxisomal function. The loss of Pex5 demonstrated a robust suppression of peroxisomal

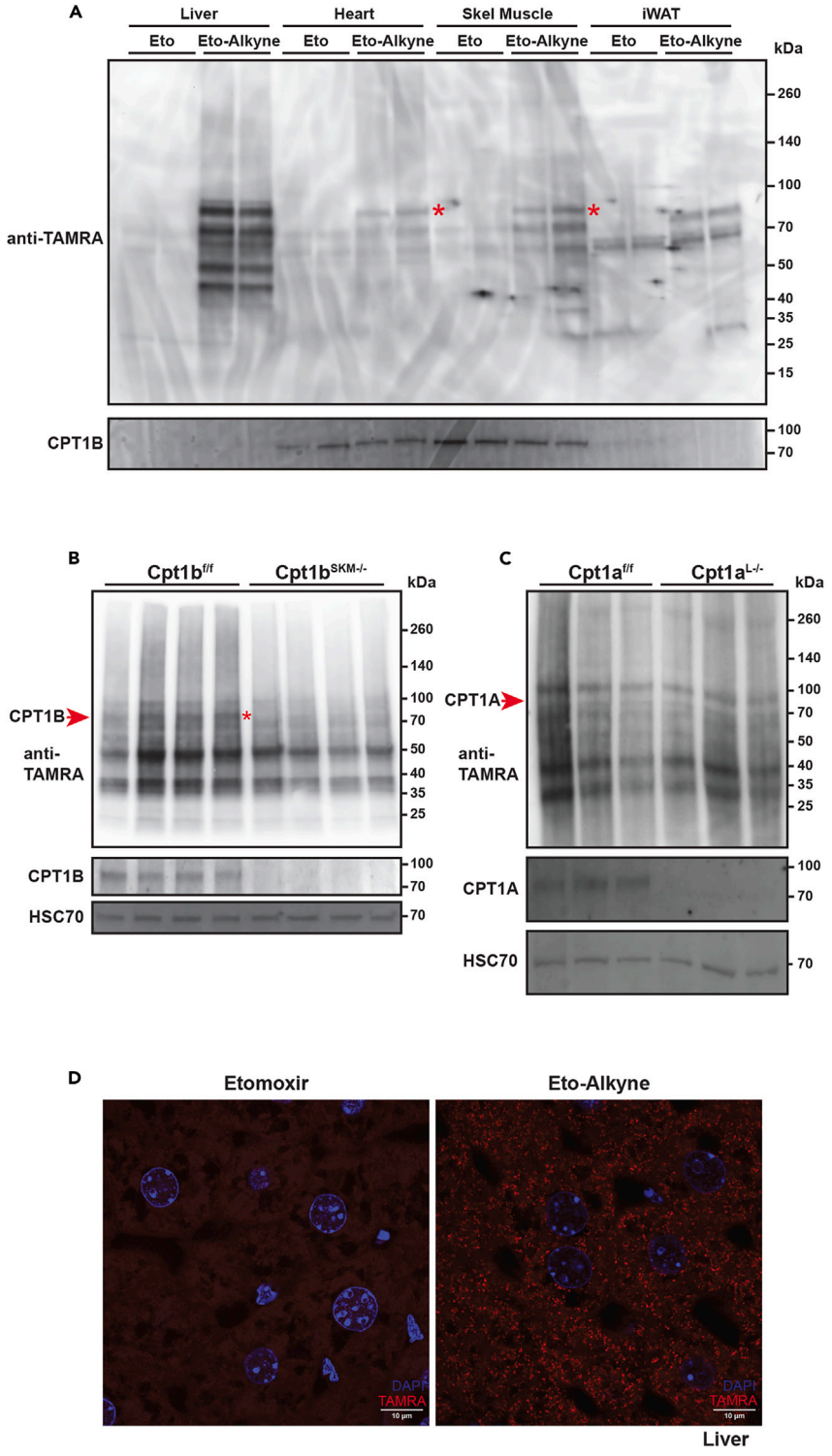

Figure 2. Click-enabled etomoxir labels proteins *in vivo*

(A) 3 mg/kg etomoxir or etomoxir-alkyne was injected intraperitoneally over three days. The on-target Cpt1b can be visualized in heart and skeletal muscle via Western blot.

(B) 3 mg/kg etomoxir-alkyne was injected IP over three days into control Cpt1b floxed mice or skeletal muscle specific KO of Cpt1b.

(C) 3 mg/kg etomoxir-alkyne was injected IP over three days into control Cpt1a floxed mice or liver specific KO of Cpt1a.

(D) Localization of etomoxir-alkyne (red) in the liver of wild-type mice injected with etomoxir or etomoxir-alkyne intraperitoneally. Scale bar: 10μm.

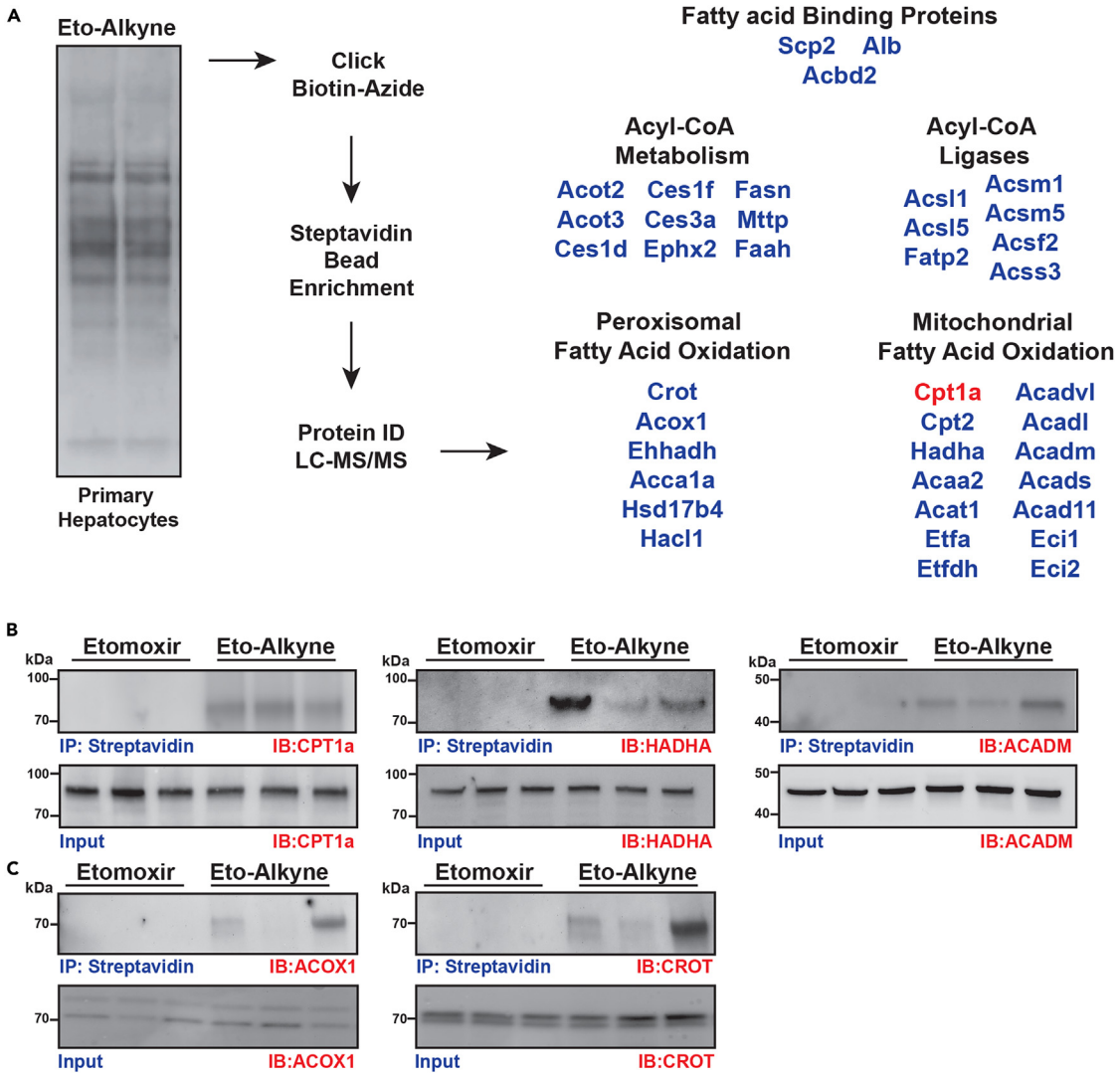

Figure 3. Proteomic identification of etomoxir binding proteins

(A) Workflow of proteomics identification including proteins identified in primary hepatocytes.

(B) Follow up immunoprecipitation-Western blots for Eto-Alkyne bound mitochondrial proteins.

(C) Follow up immunoprecipitation-Western blots for Eto-Alkyne bound peroxisomal proteins.

etomoxir binding proteins by SDS-PAGE and cellular staining (Figure S2). The punctate staining of cells and hepatocytes resembled peroxisomal rather than mitochondrial morphology. Therefore, we expressed either a peroxisomal-eGFP or mitochondrial-eYFP in primary hepatocytes. Click-etomoxir overlapped perfectly with peroxisomal-eGFP (Figure 4A). We did not observe the same level of overlap with a mitochondrially localized eYFP. Even though etomoxir inhibits mitochondrial fatty acid oxidation and binds to mitochondrial proteins, the majority of cellular localization is peroxisomal. These data again show that rather than specifically targeting mitochondria, etomoxir binds to and marks peroxisomal proteins.

Finally, we generated WT, Cpt1a KO and Pex5 KO primary hepatocytes and labeled them with Click-etomoxir. Again, even though we have shown that Cpt1a binds to and is inhibited by etomoxir, Cpt1a is not one of the top etomoxir binding proteins in hepatocytes (Figure 4B). However, the loss of Pex5 severely diminished etomoxir binding proteins as visualized by SDS-PAGE (Figure 4B). These data show that peroxisomal proteins are a major target of etomoxir. Indeed, the liver and kidney show the most etomoxir binding proteins and they have the highest peroxisomal content among the tissues we assayed likely obscuring Cpt1a. Given that Click-etomoxir is binding promiscuously to fatty acid binding proteins, we wondered if it could be used as an activity dependent fatty acid mimetic probe. Indeed, Pex5 KO hepatocytes lost many etomoxir binding proteins as expected but also gained proteins not seen in either control or Cpt1a KO hepatocytes (Figure 4B). In order to identify these new etomoxir binding proteins and the lost etomoxir binding proteins, we isolated control and Pex5 KO primary hepatocytes and performed quantitative label free proteomics (n = 4 biological replicates) on control hepatocytes labeled with etomoxir

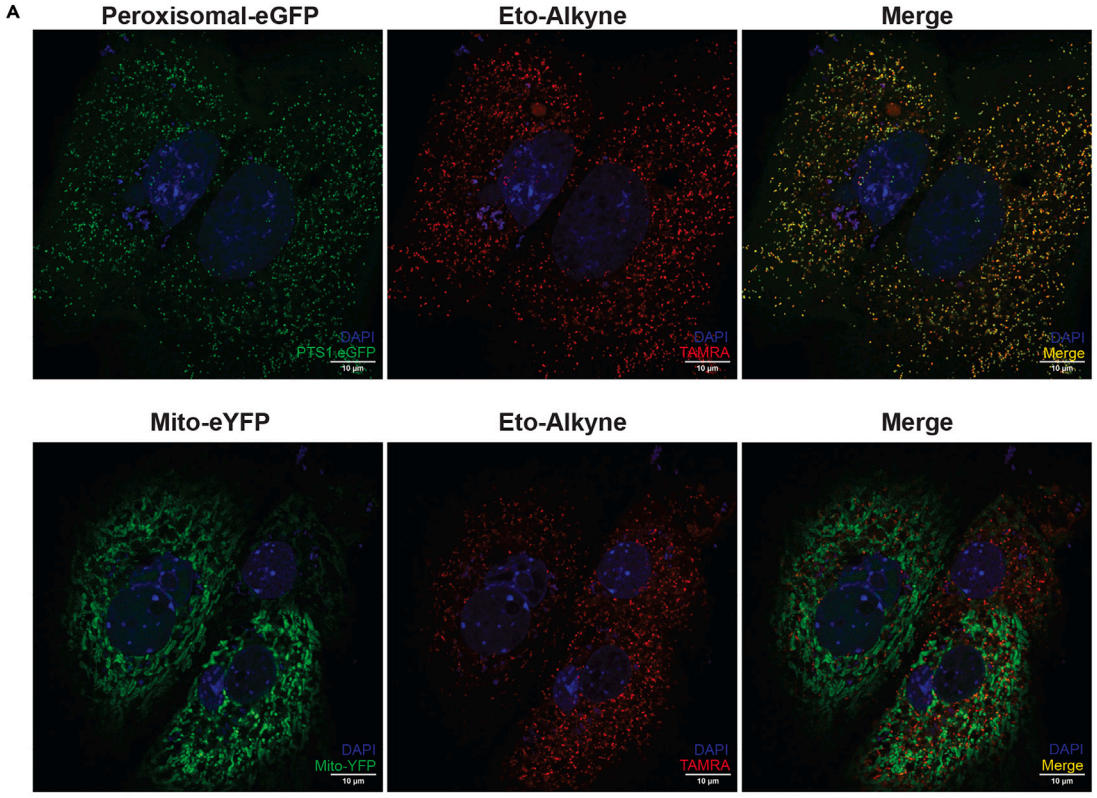

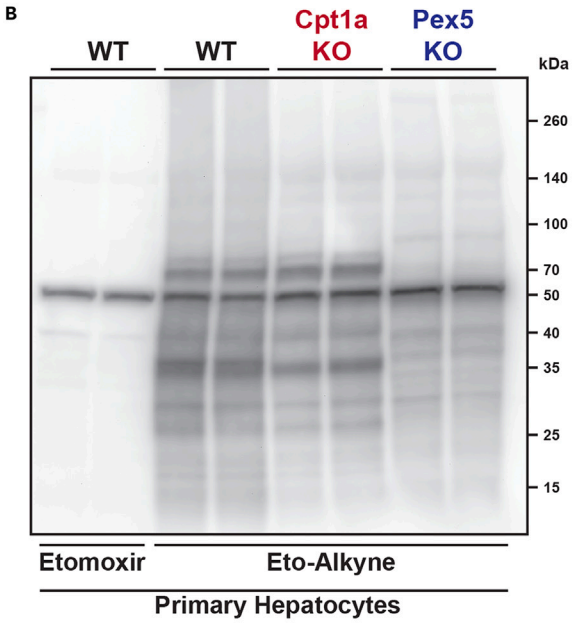

C

Pex5/WT hepatocytes

reduced (114)	unchanged (416)	enriched (92)
Acat2	Aacs	Acnat2
Acnat1	Abhd6	Cd36
Acot8	Acaa1b	Crls1
Acox1	Acat3	Cyp4a10
Cyp17a1	Acot1	Cyp4a12b
Cyp2c40	Agpat2	Cyp4a14
Cyp2c50	Apob	Cyp4f14
Cyp3a16	Ces2g	Decr2
Dbi	Ces3b	Hacl1
Lmf1	Coasy	Hmgcs1
Lmf2	Fads1	Hsd17b4
Lonp2	Gpx4	Insig2
Ndufb3	Ldhb	Khk
Ndufb8	Lpcat3	Pgk2
Ndufs3	Mboat7	Phka2
Pex16	Ndufab1	Pipox
Psmb8	Pctp	Pklr
Pxmp4	Pdk4	Plbd1
Pygb	Rras	Pon2
Slc2a2		Vps16

Figure 4. Peroxisomes are major targets of etomoxir in hepatocytes

(A) Co-localization of etomoxir-alkyne with peroxisomal or mitochondrial markers show peroxisomal puncta (green) and mitochondria (YFP) with TAMRA (red). Scale bar: 10μm.

(B) Identification of etomoxir binding proteins in control, Cpt1a KO and Pex5 KO primary hepatocytes.

(C) Proteomic identification of etomoxir binding proteins enriched, unchanged, or reduced in Pex5 KO primary hepatocytes by label free quantitative proteomics.

and control and Pex5KO hepatocytes labeled with Click-etomoxir. As predicted, numerous proteins were reduced including many peroxisomal proteins such as Acox1 in Pex5 KO hepatocytes (Figure 3C; Table S3). However, a number of proteins, for example, cytochrome P450 (Cyp4) family members were enriched specifically in Pex5 KO hepatocytes (Figure 4C). Mitochondria and peroxisomes both perform fatty acid β-oxidation with unique biochemical endpoints. However, the endoplasmic reticulum can also participate in the more enigmatic ω-oxidation and Cyp4 enzymes initiate this less prominent fatty acid degradative pathway. These data show that etomoxir can be used to discover fatty acid binding proteins under unique physiologic or pathologic conditions.

DISCUSSION

Etomoxir is one of the most utilized small molecule inhibitors in all of metabolic research. It is often described as a Cpt1 specific inhibitor used to distinguish the biological effects of mitochondrial fatty acid β-oxidation. Clearly, this is inappropriate given the sheer number of proteins it binds. In fact, there has never been a test of its specificity and it is unclear where this idea propagated from. Moving forward it is not clear that there are any small molecule inhibitors of fatty acid oxidation that would fit a criteria of specificity and efficacy.[12] One possible method to demonstrate specificity is to rescue the effect of etomoxir by adding a medium chain fatty acid such as octanoate (C8:0) that enters mitochondria in a Cpt1 independent manner.[13] However, not all cells express the enzymes required for octanoate oxidation.[14] For cell culture, chemical genetic regulation of proteins could be used to affect function in a chemical and gene specific manner as we have done here (Figure 1B).[15,16] *In vivo*, either Crispr or KO studies are likely required to make stringent conclusions. More broadly, beyond demonstrating efficacy it is unclear how any small molecule has been thoroughly vetted for its specificity to enable rigorous fundamental discovery research. This continues to plague drug discovery while impacting thousands of patients enrolled in clinical trials.[17] Here we have the advantage of a small molecule that makes a covalent linkage to its targets. Other small molecules that interact more transiently require further method development.[18,19]

Transcriptomic, proteomic and metabolomic methods are limited in their ability to describe protein engagement and changes in enzyme activity during biological or pathobiological states. Activity-dependent chemical probes offer unique insights into the functional analysis of proteins in complex biological systems by informing the biochemical activity of proteins *in situ*.[20–24] We have taken a well-described covalent inhibitor of fatty acid oxidation and generated a Click chemistry-enabled probe that promiscuously labels enzymes in fatty acid metabolism in an activity-dependent manner *in situ*. Etomoxir's structure is similar to a fatty acid and is CoA esterified in cells. Indeed, we have captured enzymes that add CoA to fatty acids (Acsl1, Acsl5, Fatp2) with the Click-etomoxir probe. In fact, we have captured much of the fatty acid metabolic machinery in hepatocytes. Using our Click-etomoxir probe in combination with genetic manipulations (Cpt1A KO and Pex5 KO hepatocytes) and Click-etomoxir probe, we were able to observe the redistribution of fatty acid catabolism to ω-oxidation utilizing Click-etomoxir demonstrating its utility in identifying shifted biology. These experiments uncovered other proteins not known to use fatty acids and will require more in-depth experimentation. Utilizing the promiscuous and covalent binding of etomoxir should enable the discovery of unique fatty acid biology.

Research into fatty acid oxidation has been dominated for decades by the rigid notion that etomoxir solely targets mitochondrial fatty acid oxidation. This requires re-evaluation as the global impact of etomoxir on multiple metabolic pathways indicates that past conclusions are likely to be highly flawed. These data should serve as a cautionary tale and propel the development of more rigorous tools for manipulating metabolic biochemistry more broadly. While mouse knockout studies are critically important, the metabolic community is in need of new tools to manipulate metabolic pathways in a rigorous, efficacious and specific manner on a timescale uniquely provided by small molecule inhibitors.

Limitations of the study

We have rigorously shown that etomoxir binds to a myriad of proteins and used proteomics to identify the proteins that etomoxir is bound to including enzymes involved in fatty acid oxidation, a pathway that is clearly inhibited by etomoxir. However, this does not necessarily mean that etomoxir is effectively inhibiting the function of the diverse array of bound proteins. Additional functional studies are required to understand the target-specific effects that etomoxir has on target function.

STAR★METHODS

Detailed methods are provided in the online version of this paper and include the following:

- KEY RESOURCES TABLE
- RESOURCE AVAILABILITY
  - Lead contact
  - Materials availability
  - Data and code availability

SUPPLEMENTAL INFORMATION

Supplemental information can be found online at https://doi.org/10.1016/j.isci.2024.110642.

ACKNOWLEDGMENTS

We thank Robert Noland from the Pennington Biological Research Center for providing Cpt1b floxed mice. We thank Robert Cole and the Johns Hopkins Proteomics Facility. This work was supported in part by a National Institutes of Health grant R01DK120530 to M.J.W., R01NS111230 to S.S, R01AI125402 to T.J.O. and R01DK099134 to R.C.R.

AUTHOR CONTRIBUTIONS

M.J.W. and J.C. designed the experiments. J.C., D.M.S., Y.J.L., M.J.H., T.J.O., and P.D. performed the experiments and collected data. D.C., T.J.O., N.J.H., S.S., R.C.R., and M.J.W. provided key experimental equipment and technical support. J.C., D.M.S., Y.J.L., T.J.O., P.D., N.J.H., and M.J.W. analyzed the data. J.C. and M.J.W. wrote the manuscript.

DECLARATION OF INTERESTS

The authors declare no competing interests.

Received: November 15, 2023
Revised: May 17, 2024
Accepted: July 30, 2024
Published: August 2, 2024

REFERENCES

1. Houten, S.M., Violante, S., Ventura, F.V., and Wanders, R.J.A. (2016). The Biochemistry and Physiology of Mitochondrial Fatty Acid beta-Oxidation and Its Genetic Disorders. Annu. Rev. Physiol. *78*, 23–44. https://doi.org/10.1146/annurev-physiol-021115-105045.
2. O'Neill, L.A.J., Kishton, R.J., and Rathmell, J. (2016). A guide to immunometabolism for immunologists. Nat. Rev. Immunol. *16*, 553–565. https://doi.org/10.1038/nri.2016.70.
3. Mutlu, A.S., Duffy, J., and Wang, M.C. (2021). Lipid metabolism and lipid signals in aging and longevity. Dev. Cell *56*, 1394–1407. https://doi.org/10.1016/j.devcel.2021.03.034.
4. Carracedo, A., Cantley, L.C., and Pandolfi, P.P. (2013). Cancer metabolism: fatty acid oxidation in the limelight. Nat. Rev. Cancer *13*, 227–232. https://doi.org/10.1038/nrc3483.
5. Ceccarelli, S.M., Chomienne, O., Gubler, M., and Arduini, A. (2011). Carnitine palmitoyltransferase (CPT) modulators: a medicinal chemistry perspective on 35 years of research. J. Med. Chem. *54*, 3109–3152. https://doi.org/10.1021/jm100809g.
6. Nomura, M., Liu, J., Rovira, I.I., Gonzalez-Hurtado, E., Lee, J., Wolfgang, M.J., and Finkel, T. (2016). Fatty acid oxidation in macrophage polarization. Nat. Immunol. *17*, 216–217. https://doi.org/10.1038/ni.3366.
7. Gonzalez-Hurtado, E., Lee, J., Choi, J., Selen Alpergin, E.S., Collins, S.L., Horton, M.R., and Wolfgang, M.J. (2017). Loss of macrophage fatty acid oxidation does not potentiate systemic metabolic dysfunction. Am. J. Physiol. Endocrinol. Metab. *312*, E381–E393. https://doi.org/10.1152/ajpendo.00408.2016.
8. Yao, C.H., Liu, G.Y., Wang, R., Moon, S.H., Gross, R.W., and Patti, G.J. (2018). Identifying off-target effects of etomoxir reveals that carnitine palmitoyltransferase I is essential for cancer cell proliferation independent of beta-oxidation. PLoS Biol. *16*, e2003782. https://doi.org/10.1371/journal.pbio.2003782.
9. Raud, B., Roy, D.G., Divakaruni, A.S., Tarasenko, T.N., Franke, R., Ma, E.H., Samborska, B., Hsieh, W.Y., Wong, A.H., Stüve, P., et al. (2018). Etomoxir Actions on Regulatory and Memory T Cells Are Independent of Cpt1a-Mediated Fatty Acid Oxidation. Cell Metab. *28*, 504–515.e7. https://doi.org/10.1016/j.cmet.2018.06.002.
10. Divakaruni, A.S., Hsieh, W.Y., Minarrieta, L., Duong, T.N., Kim, K.K.O., Desousa, B.R., Andreyev, A.Y., Bowman, C.E., Caradonna, K., Dranka, B.P., et al. (2018). Etomoxir Inhibits Macrophage Polarization by Disrupting CoA Homeostasis. Cell Metab. *28*, 490–503.e7. https://doi.org/10.1016/j.cmet.2018.06.001.
11. O'Connor, R.S., Guo, L., Ghassemi, S., Snyder, N.W., Worth, A.J., Weng, L., Kam, Y., Philipson, B., Trefely, S., Nunez-Cruz, S., et al. (2018). The CPT1a inhibitor, etomoxir induces severe oxidative stress at commonly used concentrations. Sci. Rep. *8*, 6289. https://doi.org/10.1038/s41598-018-24676-6.
12. Ma, Y., Wang, W., Devarakonda, T., Zhou, H., Wang, X.Y., Salloum, F.N., Spiegel, S., and Fang, X. (2020). Functional analysis of molecular and pharmacological modulators of mitochondrial fatty acid oxidation. Sci. Rep. *10*, 1450. https://doi.org/10.1038/s41598-020-58334-7.
13. Sharpley, M.S., Chi, F., Hoeve, J.T., and Banerjee, U. (2021). Metabolic plasticity drives development during mammalian embryogenesis. Dev. Cell *56*, 2329–2347.e6. https://doi.org/10.1016/j.devcel.2021.07.020.
14. Pereyra, A.S., McLaughlin, K.L., Buddo, K.A., and Ellis, J.M. (2023). Medium-chain fatty acid oxidation is independent of L-carnitine in liver and kidney but not in heart and skeletal muscle. Am. J. Physiol. *325*, G287–G294. https://doi.org/10.1152/ajpgi.00105.2023.
15. Rodriguez, S., and Wolfgang, M.J. (2012). Targeted chemical-genetic regulation of protein stability *in vivo*. Chem. Biol. *19*, 391–398. https://doi.org/10.1016/j.chembiol.2011.12.022.
16. Rodriguez, S., Ellis, J.M., and Wolfgang, M.J. (2014). Chemical-genetic induction of Malonyl-CoA decarboxylase in skeletal

muscle. BMC Biochem. *15*, 20. https://doi.org/10.1186/1471-2091-15-20.

17. Lin, A., Giuliano, C.J., Palladino, A., John, K.M., Abramowicz, C., Yuan, M.L., Sausville, E.L., Lukow, D.A., Liu, L., Chait, A.R., et al. (2019). Off-target toxicity is a common mechanism of action of cancer drugs undergoing clinical trials. Sci. Transl. Med. *11*, eaaw8412. https://doi.org/10.1126/scitranslmed.aaw8412.
18. Trowbridge, A.D., Seath, C.P., Rodriguez-Rivera, F.P., Li, B.X., Dul, B.E., Schwaid, A.G., Buksh, B.F., Geri, J.B., Oakley, J.V., Fadeyi, O.O., et al. (2022). Small molecule photocatalysis enables drug target identification via energy transfer. Proc. Natl. Acad. Sci. USA *119*, e2208077119. https://doi.org/10.1073/pnas.2208077119.
19. Huth, S.W., Oakley, J.V., Seath, C.P., Geri, J.B., Trowbridge, A.D., Parker, D.L., Jr., Rodriguez-Rivera, F.P., Schwaid, A.G., Ramil, C., Ryu, K.A., et al. (2023). muMap Photoproximity Labeling Enables Small Molecule Binding Site Mapping. J. Am. Chem. Soc. *145*, 16289–16296. https://doi.org/10.1021/jacs.3c03325.
20. Barglow, K.T., and Cravatt, B.F. (2007). Activity-based protein profiling for the functional annotation of enzymes. Nat. Methods *4*, 822–827. https://doi.org/10.1038/nmeth1092.
21. Liu, Y., Patricelli, M.P., and Cravatt, B.F. (1999). Activity-based protein profiling: the serine hydrolases. Proc. Natl. Acad. Sci. USA *96*, 14694–14699. https://doi.org/10.1073/pnas.96.26.14694.
22. Martin, B.R., and Cravatt, B.F. (2009). Large-scale profiling of protein palmitoylation in mammalian cells. Nat. Methods *6*, 135–138.
23. Simon, G.M., and Cravatt, B.F. (2010). Activity-based proteomics of enzyme superfamilies: serine hydrolases as a case study. J. Biol. Chem. *285*, 11051–11055. https://doi.org/10.1074/jbc.R109.097600.
24. van Esbroeck, A.C.M., Janssen, A.P.A., Cognetta, A.B., 3rd, Ogasawara, D., Shpak, G., van der Kroeg, M., Kantae, V., Baggelaar, M.P., de Vrij, F.M.S., Deng, H., et al. (2017). Activity-based protein profiling reveals off-target proteins of the FAAH inhibitor BIA 10-2474. Science *356*, 1084–1087. https://doi.org/10.1126/science.aaf7497.
25. Wicks, S.E., Vandanmagsar, B., Haynie, K.R., Fuller, S.E., Warfel, J.D., Stephens, J.M., Wang, M., Han, X., Zhang, J., Noland, R.C., and Mynatt, R.L. (2015). Impaired mitochondrial fat oxidation induces adaptive remodeling of muscle metabolism. Proc. Natl. Acad. Sci. USA *112*, E3300–E3309. https://doi.org/10.1073/pnas.1418560112.
26. Lee, P., Peng, H., Gelbart, T., and Beutler, E. (2004). The IL-6- and lipopolysaccharide-induced transcription of hepcidin in HFE-transferrin receptor 2-and beta 2-microglobulin-deficient hepatocytes. Proc. Natl. Acad. Sci. USA *101*, 9263–9265. https://doi.org/10.1073/pnas.0403108101.
27. Hossain, M.J., and O'Connor, T.J. (2024). An efficient and cost-effective method for disrupting genes in RAW264.7 macrophages using CRISPR-Cas9. PLoS One *19*, e0299513. https://doi.org/10.1371/journal.pone.0299513.
28. Bligh, E.G., and Dyer, W.J. (1959). A rapid method of total lipid extraction and purification. Can. J. Biochem. Physiol. *37*, 911–917. https://doi.org/10.1139/o59-099.
29. Chen, S., Datta-Chaudhuri, A., Deme, P., Dickens, A., Dastgheyb, R., Bhargava, P., Bi, H., and Haughey, N.J. (2019). Lipidomic characterization of extracellular vesicles in human serum. J. Circ. Biomark. *8*, 1849454419879848. https://doi.org/10.1177/1849454419879848.

STAR★METHODS

KEY RESOURCES TABLE

REAGENT or RESOURCE	SOURCE	IDENTIFIER
Antibodies		
TAMRA	Invitrogen	MA1-041
Cpt1a	Proteintech	15184-1-AP
Cpt1b	Proteintech	22170-1-AP
Hadha	Genetex	GTX101177
Acadm	Genetex	GTX101393
Crot	Proteintech	13543-1-AP
Acox1	Proteintech	10957-1-AP
Hsc70	Santa Cruz Biotechnology	7298
Mouse-HRP	Cell Signaling Technology	7076S
Rabbit-HRP	Cell Signaling Technology	7074S
Cy3	Thermo Fisher Scientific	M30010
Bacterial and virus strains		
AAV with TBG promoter driven iCre	Vector Biolabs	VB1724
AAV with TBG promoter driven eGFP	Vector Biolabs	VB1743
Chemicals, peptides, and recombinant proteins		
Trimethoprim	Boston Bioproducts Inc.	C06K1
Etomoxir	Sigma-Aldrich	E1905
Tetramethylrhodamine (TAMRA) Azide (Tetramethylrhodamine 5-Carboxamido-(6-Azidohexanyl)), 5-isomer	Invitrogen	T10182
Tetramethylrhodamine (TAMRA) Alkyne (5-Carboxytetramethylrhodamine, Propargylamide), 5-isomer	Invitrogen	T10183
Dde Biotin Azide	Click Chemistry Tools	CCT-1136
Critical commercial assays		
Click-iT™ Protein Reaction Buffer Kit	Invitrogen	C10276
Click-iT™ Cell Reaction Buffer Kit	Invitrogen	C10269
Deposited data		
Proteome data	This Paper	ProteomeXchange: PXD045866
Proteome data	This Paper	ProteomeXchange: PXD051969
Experimental models: Cell lines		
Raw264.7 WT and Pex5KO lines	This Paper	ATCC TIB-71
HEK293T cells overexpressing Cpt1a plasmid	This Paper	N/A
Experimental models: Organisms		
Cpt1a floxed mice	Taconic Biosciences	9759
Pex5 floxed mice	Jackson Laboratories	031665
Albumin-Cre Transgenic mice	Jackson Laboratories	003574
Cpt1b floxed; Mlc1f-Cre Transgenic mice	Wicks et al., 2015[4]	N/A
Recombinant DNA		
Plasmid – Cpt1a-FLAG-DHFR	This Paper	N/A

RESOURCE AVAILABILITY

Lead contact

Further information and requests for resources and reagents should be directed to and will be fulfilled by the lead contact, Michael J. Wolfgang, Ph.D. (mwolfga1@jhmi.edu).

Materials availability

Click-etomoxir reagents were synthesized and validated by Otava Chemicals Ltd. (Ontario, Canada) and are available upon request.

Data and code availability

Proteome data has been deposited to ProteomeXchange: PXD045866 and PXD051969.

METHOD DETAILS

Animals

All animals utilized were housed in ventilated racks at a 14hr-light/10hr-dark cycle and fed a standard chow diet (2018SC Teklad global). At 9 weeks of age, male mice were injected for three consecutive days with 3 mg/kg etomoxir or 3 mg/kg etomoxir-alkyne in 0.9% saline solution. After the final injection of the compounds, mice were restricted from food for 4 h and tissues were collected. Cpt1a floxed mice (Taconic Biosciences, #9759), and Pex5 floxed mice (Jackson Laboratory #031665) were either bred to Albumin-Cre mice (Jackson Laboratory #003574) or injected with an AAV vector expressing GFP or iCre under the TBG promoter (Vector Biolabs). Cpt1b muscle specific KO mice were generated by crossing floxed *Cpt1b* mice to *Mlc1f-Cre* transgenic mice.[25] Tissues used for sectioning were fixed directly into 4% paraformaldehyde overnight and stored in 30% sucrose until embedding into O.C.T. Compound (Scigen) and sectioned into 8μm sections. Sections were permeabilized in 0.3% Triton X-100 and blocked with 5% donkey serum prior to click reaction. All procedures were done in accordance with the NIH's Guide for the Care and Use of Laboratory Animals and under the approval of the Johns Hopkins Medical School Animal Care and Use Committee.

Western blots

Cell lysate and tissue homogenate was prepared in 1x RIPA buffer with protease and proteinase inhibitors. Protein concentration was measured using the Pierce BCA Protein Assay Kit (Thermo Scientific) and 100-200μg of protein was utilized for click reactions. 30μg of protein was loaded and ran on an SDS-PAGE and then transferred to a polyvinylidene difluoride (PVDF) membrane. Membranes were blocked with 3% BSA-TBST. Membranes were probed with antibodies TAMRA (Invitrogen), Cpt1a (Proteintech), Cpt1b (Proteintech), Hadha (Genetex), Acadm (Genetex), Crot (Proteintech), Acox1 (Proteintech) and Hsc70 as a loading control (Santa Cruz Biotechnology). Membranes were then incubated with the corresponding secondary antibodies conjugated to horseradish peroxidase with the exception of Hsc70 that used the corresponding Cy3 fluorescent secondary antibody. Membranes were imaged utilizing an Alpha Innotech FluorChemQ.

Click reaction

Click-etomoxir reagents were synthesized and validated by Otava Chemicals Ltd. (Ontario, Canada) (Figure S3). 100μg–200μg of protein were clicked to the corresponding click partner TAMRA-azide (Invitrogen), TAMRA-alkyne (Invitrogen) and Dde Biotin Azide (Click Chemistry Tools) via Click-iT Protein Reaction Buffer Kit (Invitrogen). Click-iT Cell Reaction Buffer Kit was utilized to visualize etomoxir in primary hepatocytes and RAW264.7 cells (Invitrogen). Images of primary hepatocytes and RAW264.7 cells were taken using a Zeiss LSM900 Airyscan microscope with a 63x oil objective followed by Airyscan processing (2D, default settings).

Cell culture

Primary hepatocytes were isolated following liver perfusion at a rate of 5 mL/min with buffers warmed to 44°C unless otherwise stated. Perfusion was performed with 25mL of 0.5mM EGTA in PBS, 25mL of PBS, and then 20mL of Liver Digest Media (Gibco, 17703034) supplemented with 0.15 mg/mL collagenase (Sigma, C5138) at a rate of 2 mL/min. Perfused livers were transferred to a chilled Petri dish containing 15mL Hepatocyte Wash Media (Gibco, 17704024) and dissociated. The dissociated cells were then pelleted at 50xg for 5min and washed twice with wash media. The washed hepatocytes were resuspended with 25mL Media 199 (Gibco, 11150059) and mixed with 20mL Percoll (Sigma, GE17-0891-01). Hepatocytes were pelleted at 300xg for 10min and then washed once more with 15mL Media 199 prior to plating.[26] Cells were treated with DMSO, 100μM etomoxir or 100μM etomoxir alkyne/azide for 14 h and harvested for subsequent click chemistry and western blotting. To compete off etomoxir in Figure 1G, cells were pre-treated for 12 h with different concentrations of etomoxir, washed with 1xPBS and then treated for 2 h with 0.1μM etomoxir-alkyne and harvested. A plasmid encoding a Cpt1a-FLAG-DHFR fusion protein was inserted into a pcDNA-3.1 backbone by standard cloning procedures. Stably expressing Cpt1a-FLAG-DHFR (denoted tg-Cpt1a) HEK293T cells were selected by hygromycin resistance and maintained in DMEM (Gibco, 11995073) supplemented in 10% fetal bovine serum and 1% penicillin-streptomycin 100x solution. For dose-dependency of tg-Cpt1a expression depicted in Figure 1B, cells were incubated in the presence of 0.1, 1, 30, or 100μM trimethoprim (Boston BioProducts Inc.) or DMSO vehicle control for 24h prior to protein harvest and western blot analysis of tg-Cpt1a protein levels by western blot. For fatty acid oxidation capacity of tg-Cpt1a cells in the presence or absence of trimethoprim

and etomoxir or click reagents, tg-Cpt1a expressing HEK293T cells were seeded into T-25 flasks with or without 30μM trimethoprim for ~23h. Seeding media was replaced with media containing 0.12 μCi ^{14}C-oleic acid (Moravek Inc.) and combinations of 30μM trimethoprim, 100μM etomoxir, 100μM click reagents, or DMSO. T-25 flasks were plugged with a rubber stopper appended to a plastic well hovering above the media containing filter paper to capture $^{14}CO_2$ released. After 3h labeling period, the reaction was quenched by injecting 200μL 70% perchloric acid into the media and 150μL 1N NaOH onto the filter paper in the well. Flasks were placed in a 55°C oven for 1h ^{14}C on the dried filter paper was counted by liquid scintillation. Counts were normalized to protein from 2 flasks per condition that did not receive the radiolabel.

RAW264.7 cells (ATCC TIB-71) were cultured in RPMI 1640 (Gibco) containing 10% heat inactivated fetal bovine serum (FBS). Pex5 KO RAW264.7 cells were generated by CRISPR-Cas9-mediated genome editing.[27]

Targeted analysis: Fatty acid oxidation metabolism

Cell samples were thoroughly homogenized and estimated the protein amounts using BCA assay. Protein normalized cell homogenates were extracted for metabolomics using ice-cold methanol containing pre-spiked internal standards Lauric acid-D23 (50 ng/mL) and Lauroyl carnitine-D3 (40 ng/mL).

Chromatographic conditions

Chromatographic experiments were carried out on a Shimadzu Prominence HPLC system (Shimadzu, Columbia, MD, USA) consisted of an autosampler, column heater compartment, degasser and Pumps. Octadecylsilane, C_{18} (2.6μm, 50 × 2.1mm) (Phenomenex, Torrance, CA, USA) was used at 50°C for the separation of fatty acids, and fatty acylcarnitines. The autosampler (Shimadzu SIL-20AC) was maintained at 15°C and 10 μls of each sample extraction solution was injected for the analysis. A binary gradient mobile phase program was optimized for the separation of fatty acids and fatty acylcarnitines. Mobile phase-B consisted of methanol (100%) containing 10 mM ammonium formate and mobile phase-A consisted of methanol: water (37:63, v/v) containing 10mM ammonium formate. The initial B concentration was kept at 30%. A linear gradient was used as follows: 0.1 min 30%B; 4.0 min 100%B; 8 min 100%B; 9 min 30%B; 10 min stop, at a flow rate of 0.4 mL/min. The total run time for each sample run was 10 min.

Mass spectrometric conditions

Tandem mass spectrometric (MS/MS) analysis were performed on a quadrupole ion trap mass spectrometer (API 4000- Q TRAP, Applied Biosystems, Foster City, CA, USA)- equipped with a Turbo Ion Spray (TIS) source. The data were acquired (using Analyst version 1.5.1) in negative electrospray ionization for fatty acids, and dicarboxylic acids, and positive electrospray ionization for fatty acylcarnitines. All the analytes were detected in pseudo multiple reaction monitoring (MRM) mode, and the data were processed and quantified using MultiQuant 1.3. Each analyte response was normalized to its corresponding internal standard response, and these normalized values were used for statistical analysis.

Untargeted analysis: Full scale lipidomics

A crude lipid fraction was extracted from cell samples using Bligh and Dyer procedure.[28,29] In brief, 200μL of cell homogenates were gently mixed in a glass vial with ddH2O (to make up 1mL suspension) and 2.9mL methanol/dichloromethane (2:0.9, v/v) containing the following twelve internal standards: Cer d18:1/12:0 -6 ng/mL, SM d18:1/12:0–0.5 ng/mL, GlcCer d18:1/12:0–3.0 ng/mL, LacCer 18:1/12:0–10.0 ng/mL, d5-DAG d16:0/16:0 -15 ng/mL, d5-TAG 16:0/18:0/16:0 -2 ng/mL, cholesteryl-d7 ester 16:0 -30 ng/mL, PA d12:0/12:0 -500 ng/mL, PC 12:0/12:0–0.2 ng/mL, PE d12:0/12:0 -2 ng/mL, PG d12:0/12:0 -200 ng/mL, PS d12:0/12:0 -900 ng/mL. To obtain a biphasic mixture, an additional 1mL of ddH2O and 900μL dichloromethane was added and vortexed. The resultant mixture was incubated on ice for 30 min and centrifuged (10 min, 3000g, 4°C) to separate the organic and aqueous phases. The organic phase was removed and stored at −20°C. Just prior to analysis 1mL of the organic layer was dried using a nitrogen evaporator and re-suspended in 150μL of running solvent (dichloromethane:methanol (1:1) containing 5mM ammonium acetate), and 5 mg/mL of ceramide C17:0 used to track instrument performance. Lipid analysis was conducted in MS/MS^{ALL} mode on a TripleTOF 5600 (AB Sci-ex, Redwood City, CA) time of-flight mass spectrometer (TOF MS). Samples (50μL injection volume) were direct infused by HPLC at a constant flow rate of 7 μL/min using an LC-20AD pump and SIL-20AC XR autosampler (Shimadzu, Canby, OR). The mass spectrometer was operated at a mass resolution of 30,000 for time of flight (TOF) MS scan and 15,000 for product ion scan in the high sensitivity mode, and automatically calibrated every 10-sample injections using APCI positive calibration solution delivered via a calibration delivery system (AB SCIEX). The TOF MS and MS/MSALL data obtained were post aligned to internal standards using Analyst TF 1.8 (AB Sciex) with mass error less than 5 ppm. LipidView (version 1.3, AB SCIEX, Concord, Ontario, Canada AB Sciex) database was used for the identification and annotation of lipid species based on the precursor and fragment matchings from the experimental pooled sample runs. Lipid identifications were validated using a pooled cell samples extract analysis.[29] These pre-validated lipid species were then quantified in each experimental sample using MultiQuant software (version 3.0, AB Sciex, Concord, ON, Canada). Each lipid species response was normalized to its corresponding internal standard response, and these normalized values were used for statistical analysis.

Pulldowns and proteomics

Etomoxir or etomoxir-alkyne treated cells were harvested and pre-cleared for biotinylated proteins to improve specificity for subsequent pulldowns by incubation with magnetic streptavidin beads overnight. 200ug of pre-cleared cell lysate was then clicked to corresponding click

partner (Dde Biotin Azide) and incubated overnight with magnetic streptavidin beads (New England BioLabs). Beads were washed 3 times with 1% SDS, 8M urea, 20% acetonitrile and 1xPBS with proteinase and phosphatase inhibitors. 100ul of 100mM Triethyl Ammonium Bicarbonate (TEAB, pH 8) was added to the solution containing the streptavidin beads, which were then reduced with 50mM Dithiothreitol at 60°C for 45 min and subsequently alkylated with 100 mM Iodoacetamide at room temperature in the dark for 15 min. The samples were then digested on the beads by adding 8 μg of Trypsin/LysC (1:50 enzyme:protein) mixed protease (Pierce) and incubating overnight at 37°C and 1000 rpm. The digested peptides were removed by placing the tubes containing the beads on a magnetic rack. The peptides were further processed to remove detergents and background components using Sera-Mag beads (GE Healthcare GE24152105050350) and standard SP3 peptide cleanup protocols. Samples were injected using a Thermo *NEO* nano-LC and autosampler (Thermo Fisher, San Jose) onto a house packed trap and column. Trapping was performed using a 2cm x 75um 5um particle C18 column at 4ul/minute before switching flow onto a nano LC analytical column 25cm x 75um 2.4um particle. Trap and analytical column phase were ReproSil-Pur 120 C18-AQ (Dr. Maisch Ammerbuch Germany) with their respective particle sizes. Gradient elution of the peptides into an Orbitrap Exploris 480 mass spectrometer (Thermo Fisher, San Jose) was performed at 300 nl/min over 90 min with mobile phase composition changing from 2% to 90% acetonitrile in 0.1% formic acid over the length of the gradient. Thermo Lumos Orbitrap or Orbitrap Exploris MA10883C Mass spectrometry settings were 120,000 resolution for MS1 precursors and 30,000 for MS2 fragment ions with a 3 s cycle time between precursors. AGC for MS2 was set to 200% (1e5) with a maximum injection time of 54ms and a normalized collision energy of 34. For streptavidin pulldown data depicted in proteomic identification of etomoxir binding proteins, the data was searched against the Uniprot UP589 *Mus musculus* database with variable modification allowed for deamidation on NQ, oxidation on M, and phosphorylation on STY and carbamidomethyl set to static on C. Precursor and fragment ion mass tolerance were set to 5 and 10 ppm, respectively. One missed cleavage with trypsin as the enzyme was allowed. Data was then imported into Scaffold for comparison between treatments. Data were reported at 1% false discovery rate.

For label-free proteomics, raw files from mass spectrometry runs were searched by a label-free quantitation workflow in Proteome Discoverer (Thermo Scientific, version 3.1.0.638) against the Uniprot UP589 *Mus musculus* database using the CHIMERYS identification node prediction model inferys_3.0.0_fragmentation with variable modification allowed for deamidation on NQ, oxidation on M, and phosphorylation on STY and carbamidomethyl set to static on C. Precursor and fragment ion mass tolerance were set to 5 and 10 ppm, respectively. One missed cleavage with trypsin as the enzyme was allowed. Data was filtered for proteins with at least 2 peptides. Statistically significantly enriched proteins were retained only if the proteins were found in at least 2 of the 4 replicates. statistical significance is reported as the adjusted *p*-value using the Benjamini-Hockberg correction for the false discovery rate.

QUANTIFICATION AND STATISTICAL ANALYSIS

All data in Figures 1B and 1D is shown as mean values ± SEM. Statistical analysis is performed with one-way ANOVA and significance is shown as $*p < 0.05$; $**p < 0.01$; $***p < 0.001$. WT DMSO vs. treatments; $\#\#\#p < 0.001$. Cpt1aKO DMSO vs. Etomoxir.